# Rheological Properties of Associative Star Polymers in Aqueous Solutions: Effect of Hydrophobe Length and Polymer Topology

**ARTICLE** *in* MACROMOLECULES · MARCH 2009

Impact Factor: 5.8 · DOI: 10.1021/ma801805q

# Rheological Properties of Associative Star Polymers in Aqueous Solutions: Effect of Hydrophobe Length and Polymer Topology

**Sami Hietala,*,† Satu Strandman,† Paula Järvi,† Mika Torkkeli,‡ Katja Jankova,§ Søren Hvilsted,§ and Heikki Tenhu†**

*Laboratory of Polymer Chemistry, Department of Chemistry, University of Helsinki, P.O. Box 55, FIN-00014 Helsinki, Finland; Department of Physical Sciences, University of Helsinki, P.O. Box 64, FIN-00014 Helsinki, Finland; and Danish Polymer Center, Department of Chemical and Biochemical Engineering, Technical University of Denmark, Building 423, DK-2800 Kgs. Lyngby, Denmark*

*Received August 7, 2008; Revised Manuscript Received January 9, 2009*

ABSTRACT: Rheological properties of aqueous solutions of well-defined four-armed amphiphilic star block copolymers, poly(acrylic acid)-*block*-polystyrene (PAA-*b*-PS)$_4$, were investigated as a function of the length of the PS blocks, polymer concentration, and temperature and compared with a corresponding triblock copolymer. These polymers, synthesized by atom transfer radical polymerization (ATRP), were found to form hydrogels due to intermolecular association originating from the PS blocks. The increasing length of the PS block was observed to lead to more elastic networks due to increased hydrophobic interaction. Polymers bearing shorter PS blocks gave gels with relatively long linear response followed by strain hardening before shear thinning while the longer PS blocks lead to formation of elastic but brittle gels with limited linear regime before shear thinning. Star-block copolymers showed more elastic behavior compared with a triblock copolymer of comparable molar mass and composition. In small-angle X-ray scattering measurements the increasing lengths of the PS blocks were observed to lead to a shift in the scattering maxima toward lower $q$-values. Both rheological and X-ray characterization showed that the thermal properties of the gels are changed by increasing the PS block lengths. Gels with short PS blocks soften upon heating at lower temperatures compared with the gels with longer PS blocks.

## Introduction

Water-soluble polymers bearing hydrophobic groups, so-called stickers, either at the end of hydrophilic chains or grafted as pendant groups along the chains are known as associative polymers.[1−5] In aqueous solutions, the hydrophobes induce self-assembly into aggregates comparable to surfactant micelles and the hydrophobes act as transient junctions and connect different aggregates depending on concentration. Above a threshold concentration corresponding to the formation of a three-dimensional reversible network, the solutions behave as physical gels. The viscosity of such gels is higher by several orders of magnitude than that of solutions made with unmodified polymers of same molecular weight and at the same concentration. The major challenge so far has been to describe, understand, and predict the relationships between the polymer structure and the rheology of their solutions and gels.

The physical hydrogel structures found in nature as well as their various applications as thickeners has inspired the development of a number of different synthetic associative polymers. Among these are hydrophobically modified poly(ethylene oxide)s[6−13] or polyacrylamides[14−16] as well as various polyelectrolytes[17−34] or thermally responsive polymers.[34−38] The polymers associate either due to the incorporated hydrophobic comonomers or, in the case of polyelectrolytes and thermally responsive polymers, by change of external conditions making parts of the polymers to prefer interchain associations in solutions. The associative behavior can naturally be achieved also utilizing modified natural polymers or monomers, such as hydrophobically modified hydroxyethyl cellulose[39,40] or co-polypeptides.[41]

* Corresponding author: e-mail sami.hietala@helsinki.fi, tel +358919150333, fax +358919150330.
† Department of Chemistry, University of Helsinki.
‡ Department of Physical Sciences, University of Helsinki.
§ Technical University of Denmark.

The occurrence and strength of the hydrogels relying on physical interactions are susceptible to a number of parameters. In addition to the solvent medium, e.g., its pH, ionic strength, or additives used, temperature, nature of the monomers, and the distribution, length, and ratio of the hydrophobic and hydrophilic parts play an important role. We have earlier studied a 4-armed starlike amphiphilic block copolymer comprising of poly(acrylic acid) inner blocks and short polystyrene (PS) stickers (average degree of polymerization, DP, 6) at the end of the chain arms.[33] This polymer formed hydrogels at concentrations above 22 g/L at room temperature, and the resulting gels were found to respond to temperature and ionic strength. In the present study we concentrate on the effect of changing the hydrophobic−hydrophilic balance by increasing the size of the hydrophobic polystyrene sticker to DP = 15, 17, and 20. By doing this, we aim to clarify the effect of the size of the hydrophobic stickers on the structure and properties of the resulting gels. Additionally, a triblock copolymer with a comparable PAA−PS ratio and molar mass is analyzed to evaluate the effect of polymer topology on the rheological properties.

## Experimental Section

*tert*-Butyl acrylate and styrene (both from Aldrich) were distilled from $CaH_2$ prior to use. 2-Bromoisobutyryl bromide, *N,N,N,N″,N″*-pentamethyldiethylenetriamine (PMDETA), trifluoroacetic acid (TFA), and CuBr (all from Aldrich) were used without further purification. Triethylamine (Fluka) was dried with molecular sieves and distilled. Ethylene glycol (VWR International) was dried with $MgSO_4$ and distilled. THF (Laboratory-Scan) was dried with molecular sieves.

A linear poly(styrene)-*block*-poly(acrylic acid)-*block*-poly(styrene) triblock copolymer, PS-*b*-PAA-*b*-PS, and the starlike poly(acrylic acid)-*block*-poly(styrene) diblock copolymers, (PAA-*b*-PS)$_4$, were synthesized by atom transfer radical polymerizations of *tert*-butyl acrylate (tBA) and styrene (S), followed by the hydrolysis of *tert*-butyl ester groups with trifluoroacetic acid. The starlike polymers

10.1021/ma801805q CCC: $40.75 
Published on Web 02/11/2009

**Scheme 1. Synthesis of Starlike Amphiphilic Block Copolymers, (PAA-*b*-PS)$_4$**

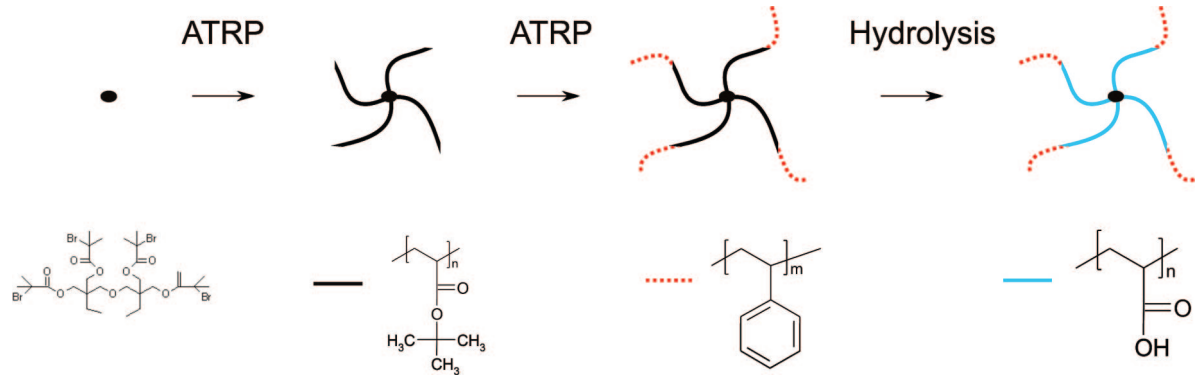


**Table 1. Molar Masses of the Investigated Starlike and Linear Block Copolymers**

| polymer | $M_n$(SEC,RI),[a] g/mol | $M_w/M_n$[b] | $M_n$(NMR),[c] g/mol |
|---|---|---|---|
| (PAA$_{54}$-*b*-PS$_6$)$_4$ | 23 500 (0.97) | 1.15 | 23 100 |
| (PAA$_{64}$-*b*-PS$_{15}$)$_4$ | 30 300 (0.95) | 1.25 | 31 100 |
| (PAA$_{64}$-*b*-PS$_{17}$)$_4$ | 31 400 (0.96) | 1.26 | 32 000 |
| (PAA$_{58}$-*b*-PS$_{20}$)$_4$ | 25 400 (0.97) | 1.09 | 30 900 |
| PS$_{27}$-*b*-PAA$_{139}$-*b*-PS$_{27}$ | 25 900 (0.97) | 1.48 | 19 200 |

[a] Calculated from the $M_n$(SEC) of the unhydrolyzed precursor using the degree of hydrolysis given by $^1$H NMR (in parentheses). [b] From SEC. [c] Calculated from the $M_n$(NMR) of the unhydrolyzed precursor using the degree of hydrolysis given by $^1$H NMR.

were prepared as described earlier[33] using a tetrafunctional 2-bromoisobutyryl derivative of di(trimethylolpropane) (diTMP-Br) as an initiator.[42] Instead of molar masses, we use the number of respective repeating units per arm for the star polymers; thus, the sample with a code (PAA$_{54}$-*b*-PS$_6$)$_4$ stands for a four-armed star polymer with arms having 54 acrylic acid units and 6 styrene units per arm. The numbers of arms (functionalities *f*) determined by the end-group analysis from $^1$H NMR spectra of the starlike poly(*tert*-butyl acrylate) macroinitiators[33] were $f = 4.05$ for (PtBA$_{54}$)$_4$ (described in ref 33), $f = 4.09$ for (PtBA$_{64}$)$_4$, and $f = 4.03$ for (PtBA$_{58}$)$_4$. Scheme 1 shows the synthesis route to starlike amphiphilic block copolymers, and their molar masses are summarized in Table 1. A more detailed description of the precursors is provided in the Supporting Information. The synthesis of a linear polymer by a difunctional initiator, ethylene glycol bis(2-bromoisobutyrate), is described below.

**Synthesis of Difunctional Initiator.** The procedure described by Matyjaszewski et al.[43] for the synthesis of difunctional initiator, ethylene glycol bis(2-bromoisobutyrate), was adapted. Ethylene glycol (5.0 g, 80.6 mmol) and triethylamine (33.8 mL, 0.24 mol) were mixed in 500 mL of tetrahydrofuran, and the solution was cooled to 0 °C. 2-Bromoisobutyryl bromide (29.9 mL, 0.24 mol) in 50 mL of THF was added dropwise for 1 h to the reaction mixture, after which it was stirred at room temperature for 24 h. The mixture was filtered and concentrated with a rotary evaporator. The concentrate was dissolved in dichloromethane (300 mL) and washed with 7 × 300 mL of $H_2O$, 1 × 300 mL of concentrated $NaHCO_3$, and again with 1 × 300 mL of $H_2O$. The organic phase was dried over $MgSO_4$, and the solvent was removed with a rotary evaporator. The product was distilled and purified by crystallization and recrystallization in hexane, giving white needle-like crystals. $^1$H NMR (200 MHz, $CDCl_3$) $\delta$ ppm: 4.44 (4 H, $CH_2$), 1.95 (12 H, $CH_3$). $^{13}$C NMR (200 MHz, $CDCl_3$) $\delta$ ppm: 171.66 (2 C, $\rangle C{=}O$), 63.40 (2 C, $CH_2$), 55.54 (2 C, $-C(CH_3)_2Br$), 30.89 (4 C, $-CH_3$). FT-IR (solid, ATR) cm$^{-1}$: 3003 (w), 2977 (w, $-CH_3$), 2929 (w, $-CH_2-$), 1721 (s, $\rangle C{=}O$), 1459 (m), 1452 (m), 1400 (w), 1387 (w), 1372 (m), 1285 and 1266 (s, $-COOR$), 1149 (s, $-COOR$), 1099 (s), 1066 (w), 1042 (m), 1021 (m), 961 (w), 944 (w), 930 (w), 890 (w), 876 (w), 866 (m), 831 (w), 816 (m), 761 (m).

**Synthesis of Linear Poly(*tert*-butyl acrylate), PtBA.** Ethylene glycol bis(2-bromoisobutyrate) (0.18 g, 0.49 mmol), *tert*-butyl acrylate (10.01 g, 78.0 mmol), CuBr (0.14 g, 0.98 mmol), and PMDETA (211 $\mu$L, 0.98 mmol) were placed in a dry flask equipped with a magnetic bar and an adapter with a high-vacuum valve. The system was degassed under vacuum in a Schlenk line by three freeze−thaw cycles. The polymerization was conducted at 70 °C for 40 min, after which it was terminated by immersing the flask into liquid nitrogen and adding some THF into the reaction mixture. The copper salts were removed by passing the solution through a column of alumina (1/5) and silica (4/5). The solvent was evaporated, and the polymer was precipitated in a mixture of MeOH and water (volume ratio 4:1). The dried polymer was further purified by reprecipitation. The molar mass determined by SEC, $M_n$(SEC), was 19 600 g/mol, and the corresponding polydispersity index was 1.13. The molar mass determined by $^1$H NMR from the signals of the initiator at 3.75 ppm (2 H, $-CH_2-$) and poly(*tert*-butyl acrylate) at 2.23 ppm (1H, $-CH_2CH-$), $M_n$(NMR), was 18 200 g/mol. $^1$H NMR (200 MHz, $CDCl_3$) $\delta$ ppm: 4.25 (br, 2 H) and 3.75 (t, 2 H, $-CH_2-$, initiator), 2.23 (1 H, $-CH-$), 1.84 and 1.76 (2 H, $-CH_2-$), 1.67, 1.44, and 1.22 (9 H, $-C(CH_3)_3$), 1.14 (9 H, $-C(CH_3)$, end group), 0.89. FT-IR (solid, ATR) cm$^{-1}$: 2997 (w), 2977 (w, $-CH_3$), 2933 (w), 2875 (w, $-CH_3$), 1723 (s, $\rangle C{=}O$), 1479 (w, $-CH_3$), 1448 (w), 1392 (m), 1366 (m, $-CH_3$), 1335 (w), 1253 (m, $\rangle C{=}O$), 1141 (s, $-COOR$), 1034 (w), 927 (w), 909 (w), 844 (m), 811 (w), 751 (w).

**Synthesis of Linear Poly(styrene)-*block*-poly(*tert*-butyl acrylate)-*block*-poly(styrene), PS-*b*-PtBA-*b*-PS.** The block copolymerization of styrene was carried out in bulk. Linear poly(*tert*-butyl acrylate) (1.00 g, 51.0 $\mu$mol) was dissolved in styrene (4.03 g, 38.7 mmol). CuBr (29.2 mg, 0.20 mmol) and PMDETA (44.0 $\mu$L, 0.20 mmol) were added, and the system was degassed by three freeze−thaw cycles under vacuum. The polymerization was conducted at 110 °C for 20 min, after which it was terminated and precipitated as above. The molar mass determined by SEC, $M_n$(SEC), was 29 500 g/mol, and the corresponding polydispersity index was 1.56. The polystyrene content of the block copolymer, 23.8 mol %, was calculated using the aromatic signals of the polystyrene block at 6.2−7.2 ppm (5 H) and the signal of poly(*tert*-butyl acrylate) at 2.23 ppm (1 H, $-CH_2CH-$), which gave $M_n$(NMR) = 23 800 g/mol. $^1$H NMR (200 MHz, $CDCl_3$) $\delta$ ppm: 7.09 and 6.60 (5 H, Ar), 4.25 (br, 2 H) and 3.76 (t, 2 H, $-CH_2-$, initiator), 2.23 (1 H, $-CH-$, ptBA), 1.84 and 1.76 (1 H, $-CH-$, PS, and 4 H $-CH_2-$, ptBA and PS), 1.44 and 1.26 (9 H, $-C(CH_3)_3$), 1.14 (9 H, $-C(CH_3)_3$, end group). FT-IR (solid, ATR) cm$^{-1}$: 3002 (w), 2977 (w, $-CH_3$), 2933 (w), 2875 (w, $-CH_3$), 1723 (s, $\rangle C{=}O$), 1479 (w, $-CH_3$), 1448 (m), 1392 (m), 1366 (m, $-CH_3$), 1335 (w), 1253 (m, $\rangle C{=}O$), 1141 (s, $-COOR$), 1034 (w), 927 (w), 909 (w), 844 (m), 802 (w), 751 (w), 699 (w, Ar).

**Preparation of Amphiphilic Poly(styrene)-*block*-poly(acrylic acid)-*block*-poly(styrene), PS-*b*-PAA-*b*-PS.** Block copolymer was dissolved in dry $CH_2Cl_2$, and the solution was flushed with nitrogen for 10 min prior to the addition of trifluoroacetic acid (5 equiv to the *tert*-butyl ester). The mixture was stirred at room temperature for 24 h. The solution was evaporated into dryness, and the PS-*b*-PAA-*b*-PS polymer was redissolved in a mixture of acetone and water. The polymer was dialyzed in a water−acetone mixture

(3:1), followed by the dialyses in 0.05 M NaOH solution and in pure water. After the purification, the solution was frozen and subsequently freeze-dried at ambient temperature. The presence of −OH groups in the purified amphiphile was clearly observed as a broad band at $\nu = 3311$ cm$^{-1}$ in the FT-IR spectrum. The degree of hydrolysis was estimated from the $^1$H NMR spectrum of the amphiphile in $D_2O$, being 97% of the *tert*-butyl ester groups. Using this degree of hydrolysis, the molar mass of the amphiphilic block copolymer was 25 900 g/mol when calculated from the $M_n$(SEC) and 19 200 g/mol when calculated from the $M_n$(NMR) (Table 1). $^1$H NMR (200 MHz, $D_2O$) $\delta$ ppm: 7.27 and 6.85 (5 H, Ar), 2.12 (1 H, −CH−, PAA), 1.52, 1.22, and 1.12 (8 H, $-CH_2-$ PAA, ptBA, and PS as well as −CH− PS and ptBA), 1.43 (9 H, $-C(CH_3)_3$, ptBA). FT-IR (solid, ATR) cm$^{-1}$: 3311 (br, m, −COOH), 3022 (w), 2948 (w), 2902 (m), 2831 (w), 2511 (br, w), 1688 (m, ⟩C═O), 1556 (s, $-COO^-$), 1493 (w), 1451 (m), 1404 (s, $-COO^-$), 1321 (br, −COOH), 1261 (m, ⟩C═O), 1168 (w), 1094 (w), 1067 (w), 1028 (w), 944 (w), 915 (w), 845 (w), 816 (w), 792 (w), 755 (w), 698 (m, Ar).

**Methods.** The SEC analyses were performed with a Waters instrument equipped with a Styragel guard column, 7.8 × 300 mm Styragel capillary column, and Waters 2487 UV and Waters 2410 RI detectors. THF or chloroform was used as an eluent with a flow rate 0.8 mL/min. The calibration was performed either with poly(styrene) or with poly(methyl methacrylate) standards from PSS Polymer Standards Service GmbH. The conversions of the polymerizations as well as the compositions of the initiator and the polymers were determined with a Varian Gemini 2000 NMR spectrometer operating at 200 MHz for $^1$H NMR and at 50.3 MHz for $^{13}$C NMR. The chemical shifts are presented in part per million downfield from the internal TMS standard or with respect to a solvent resonance line. The IR spectra were measured from solid samples with a Perkin-Elmer Spectrum One FT-IR spectrometer.

Rheological measurements were carried out with a TA Instruments AR2000 stress-controlled rheometer. A 40 mm aluminum 1° cone and a Peltier heated plate were used for the oscillatory and steady shear measurements. The linear viscoelastic regime was established by oscillatory strain sweeps using different frequencies between 0.628 and 62.8 rad/s. Dynamic oscillatory sweeps were made in linear regime at 20 °C. Steady shear measurements were similarly made at 20 °C, and possible hysteresis of the flow curves was tested ramping the shear rate first up, then down, and then up again. In order to probe the temperature-dependent rheological properties, heating of the samples was done with a rate of 1 °C/min at oscillation frequency ($\omega$) of 6.283 rad/s. The measuring setup was covered with a sealing lid in order to prevent evaporation during the measurement. To prepare samples for rheology and small-angle X-ray scattering, weighed amounts of freeze-dried polymer were dispersed in deionized water (ELGA PURELAB Ultra) directly to desired concentration in screw capped vials and placed in oven at 80 °C for 48 h. The hygroscopic nature of the PAANa blocks of the polymers may lead to small error in the concentration calculations in the weighing of the dried polymers, but this error is thought to be small and systematic taking into account the small variation in the block ratios of the samples. After heating, the aqueous solutions were weighed to correct for possible weight loss and let to equilibrate at room temperature for several hours before measurements. After sample loading as well as after nonlinear experiments a rest period of at least 10 min was employed in order to let the samples stabilize.

Small-angle X-ray scattering (SAXS) measurements were made with a setup using sealed anode X-ray tube (Cu target), multilayer optics with pinhole collimation, and a two-dimensional position-sensitive (HISTAR) detector. The non-saline gel-like samples were sealed in flat 1.5 mm thick cuvettes with thin Mylar films as X-ray windows. The accessible range of scattering vector $q$ varied between 0.1 and 12 nm$^{-1}$, where $q$ is calculated from the scattering angle $2\theta$ and wavelength $\lambda$ (=1.54 Å) as $q = 4\pi/\lambda \sin\theta$. The scattering data were corrected for detector response, spatial resolution, and nonsample scattering and azimuthally averaged into 1-D (radial) scattering intensity.

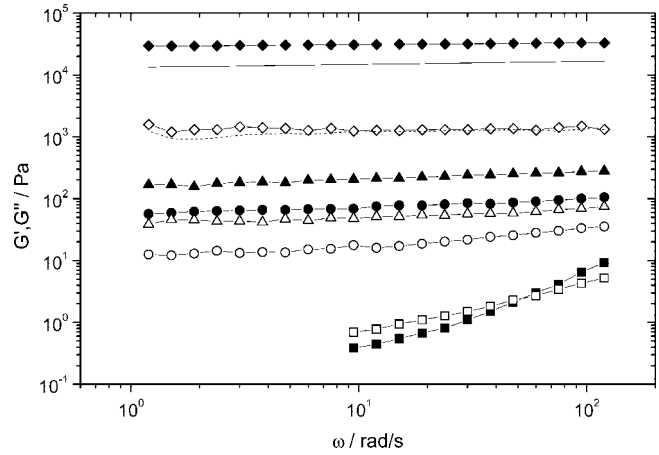


**Figure 1.** Oscillatory frequency sweeps of $(PAA_{58}$-*b*-$PS_{20})_4$ at 20 °C. Polymer concentration, $C_p$, 15 g/L ($G'$, ■; $G''$, □), 19 g/L ($G'$, ●, $G''$, ○), 20 g/L ($G'$, ▲; $G''$, Δ), 34 g/L ($G'$, ◆; $G''$, ◇) and comparison with the sample dispersed at room temperature (34 g/L; $G'$, full line; $G''$, dotted line).

## Results

**Effect of Polymer Concentration on the Rheological Properties of Aqueous Solutions.** Because of the associative nature of these amphiphilic polymers, they form viscous aqueous solutions already at relatively low concentrations and, with increasing concentration, form physical gels. The molar masses of the investigated starlike and linear amphiphilic block copolymers are summarized in Table 1. Aqueous solutions of the previously studied[33] $(PAA_{54}$-*b*-$PS_6)_4$ star polymer behaved liquid-like at polymer concentrations ($C_p$) below ∼22 g/L at 20 °C and gelled with increasing concentration. The star polymers in the present study have comparable size of the PAA polyelectrolyte core but a higher number of styrene units attached to the arms, 15 $(PAA_{64}$-*b*-$PS_{15})_4$, 17 $(PAA_{64}$-*b*-$PS_{17})_4$, or 20 $(PAA_{58}$-*b*-$PS_{20})_4$ styrene units. In order to compare the effect of polymer topology, a triblock copolymer with comparable molecular weight and composition, $PS_{27}$-*b*-$PAA_{139}$-*b*-$PS_{27}$, was studied. All the amphiphilic polymers were found to be easily dispersible to water at room temperature. However, tests with different dissolution conditions showed that heating at 80 °C for 48 h led to slightly higher modulus for the star polymer with longest PS block (PS20), and thus this heat treatment was adapted for all the solutions. To ascertain the effect of remaining (*tert*-butyl acrylate) groups (degree of hydrolysis ∼97% for all studied samples), a precursor starlike $(ptBA)_4$ polymer, $(ptBA_{64})_4$, was hydrolyzed similarly as the block copolymers, and the respective polyelectrolyte, $(PAA_{64})_4$, was studied separately.

An example of oscillatory frequency sweeps of the polymer bearing longest PS blocks is shown in Figure 1, indicating how the rheological properties of $(PAA_{58}$-*b*-$PS_{20})_4$ gradually change with increasing concentration. Figure 1 also shows how the heat treatment leads to slightly increased moduli for the sample with $C_p = 34$ g/L. Gels are obtained with increasing concentration, as shown by the moduli $G'$ exceeding $G''$ throughout the measured frequencies. With increasing concentration also a nearly frequency-independent, parallel scaling of $G'$ and $G''$ with frequency ($\omega$) is obtained, resulting in nearly frequency independent loss tangent, tan $\delta$ ($G''(\omega)/G'(\omega)$).

The increase in the length of the hydrophobe has a clear effect on the rheological properties of the resulting polymers. Compared with the $(PAA_{54}$-*b*-$PS_6)_4$, the moduli are significantly higher at the same concentration and increase monotonically with increasing PS block length. As an approximation, $G'$ at sufficient high oscillatory frequency can be taken as the plateau

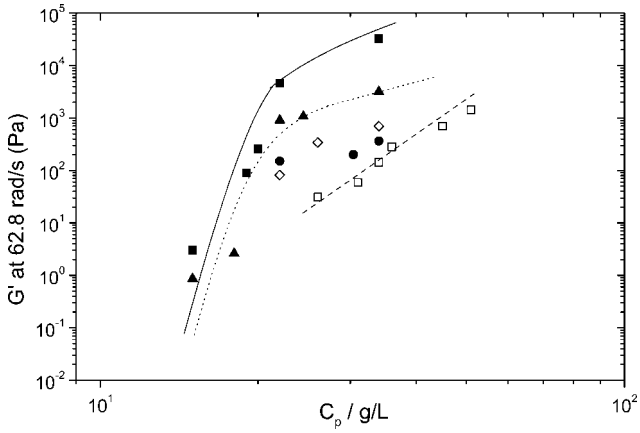


**Figure 2.** Scaling of storage modulus $G'$ at 62.8 rad/s with polymer concentration at 20 °C. Polymers $(PAA_{54}$-*b*-$PS_6)_4$ (□), $(PAA_{64}$-*b*-$PS_{15})_4$ (●), $(PAA_{64}$-*b*-$PS_{17})_4$ (▲), $(PAA_{58}$-*b*-$PS_{20})_4$ (■), and $PS_{27}-PAA_{139}-PS_{27}$ (◇). Lines are to guide the eye only. Data for $(PAA_{54}$-*b*-$PS_6)_4$ is taken from ref 33.

modulus $G_0$. We chose to use the frequency of 62.8 rad/s (10 Hz) for comparison of the storage moduli for different samples; the data are shown in Figure 2.

It was earlier found for the $(PAA_{54}$-*b*-$PS_6)_4$ that scaling relation of 5.9 between the plateau modulus and concentration existed for gel-like samples above 26 g/L, a value significantly higher than that for linear polyelectrolytes.[33] Below 26 g/L the viscosity and moduli decrease rapidly, and oscillatory measurements are complicated. Similarly as with the $(PAA_{54}$-*b*-$PS_6)_4$, the plateau modulus of the amphiphiles having longer PS blocks displays a concentration regime at which the solutions display liquid-like character; see Figure 1 for $(PAA_{58}$-*b*-$PS_{20})_4$. The increase in the length of the PS blocks only marginally affects the polymer concentration where gel-like behavior is observed, this being between 18 and 19 g/L for the polymers with PS block lengths between 15 and 20. However, the increase in PS block length induces a significant increase in the values of dynamic moduli. This difference has to be accounted for the increased hydrophobic interaction between the longer PS blocks. This conclusion is further supported by the fact that the polyelectrolyte star, $(PAA_{64})_4$, at the same mass concentrations gives only low-viscosity solution. The authors are not aware of studies where the length of a polymeric hydrophobe has been increased in a similar manner as in the present study, but it is well-known that for hydrophobically modified poly(ethylene oxide)s,[9,10] polyacrylamides,[14] or poly(acrylic acid)[18] the viscosity is enhanced with respect to increasing molar ratio[18] or block length of the hydrophobes.[15]

Further from Figure 2 it may be noted that the polymers having longer PS blocks display two ranges at which the scaling of the modulus is different. Below the threshold concentration at around 20 g/L the modulus has a very high concentration dependency, indicating the effect of quickly increasing number of transient network junctions. On the other hand, with increasing concentration the scaling factor is much smaller. Similar behavior has been observed for other hydrophobically modified polyelectrolyte and polyampholyte solutions,[12] namely to poly(*tert*-butyl acrylate)−poly(2-vinylpyridine)−poly(*tert*-butyl acrylate)) (P*t*BA-P2VP-P*t*BA) and poly(acrylic acid)−poly(2-vinylpyridine)−poly(acrylic acid) (PAA-P2VP-PAA). In steady shear experiments three distinct regions for the viscosity were seen with increasing concentration, these being a semidilute regime where viscosity increases weakly with polymer concentration, a region where a viscosity exhibits a very sharp increase over a limited concentration regime, and a regime where the viscosity increases smoothly with concentration.[12] The data in

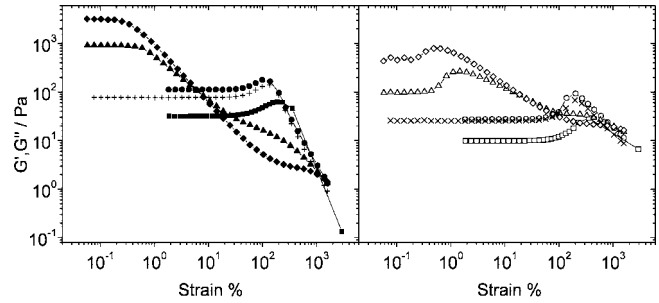


**Figure 3.** Oscillatory strain sweeps at 20 °C and oscillation frequency of 6.28 rad/s: $(PAA_{54}$-*b*-$PS_6)_4$ ($G'$, ■; $G''$, □; $C_p$ = 26 g/L); $(PAA_{64}$-*b*-$PS_{15})_4$ ($G'$, ●; $G''$, ○); $(PAA_{64}$-*b*-$PS_{17})_4$ ($G'$, ▲; $G''$, Δ), $(PAA_{58}$-*b*-$PS_{20})_4$ ($G'$, ◆; $G''$, ◇), and $PS_{27}$-$PAA_{139}$-$PS_{27}$ ($G'$, +; $G''$, ×); all $C_p$ = 22 g/L.

Figure 2 show the samples are at concentration above the "semidilute" region, and the lowest concentrations studied (15−20 g/L) for $(PAA_{58}$-*b*-$PS_{20})_4$ and $(PAA_{64}$-*b*-$PS_{17})_4$ are clearly in the sharp transition regime. For concentrations above 22 g/L the network has already developed, and a smooth increase can be noted for $(PAA_{64}$-*b*-$PS_{15})_4$, $(PAA_{64}$-*b*-$PS_{17})_4$, and $(PAA_{58}$-*b*-$PS_{20})_4$.

The effect of the polymer topology is also displayed in Figure 2, where the studied triblock copolymer, $PS_{27}$-$PAA_{139}$-$PS_{27}$, having longer PS blocks than any of the star polymers, gives intermediate plateau modulus values compared with the star polymers. The molecular weight and the composition of the triblock polymer are comparable to the star polymers. Although this does not directly imply similar size in solution, the data show that the branched starlike topology enhances the capability for intermolecular interactions and results in enhanced modulus compared with linear triblock copolymer.

**Oscillatory Strain Sweeps.** While the frequency sweeps were performed in the linear viscoelastic regime, the oscillatory strain sweeps of solutions reveals interesting characteristics. Figure 3 shows the response to increasing strain in oscillatory tests. The star polymers with shorter PS stickers, $(PAA_{54}$-*b*-$PS_6)_4$ and $(PAA_{64}$-*b*-$PS_{15})_4$, show a typical feature for associative polymer solutions,[3,7,12,17,26,39,41] the so-called strain hardening, indicated by increasing values of $G'$ at increasing strains after a linear regime, before shear thinning at higher strain. The data in Figure 3 were measured using oscillatory frequency of 6.28 rad/s. Tests with higher (62.8 rad/s) or lower (0.628 rad/s) frequencies gave the same strain values for the onset of strain hardening or shear thinning for $(PAA_{54}$-*b*-$PS_6)_4$ and $(PAA_{64}$-*b*-$PS_{15})_4$. Quite surprisingly, the star polymers with longer PS blocks, $(PAA_{64}$-*b*-$PS_{17})_4$ and $(PAA_{58}$-*b*-$PS_{20})_4$, do not behave similarly as the solutions of polymers with shorter blocks. Instead, they have a very limited range of linear response followed by strong shear thinning. It can also be seen that these solutions do exhibit a slight change of slope at higher strains, ∼10−200%. The change in slope was noted to be frequency dependent—it becomes more pronounced with higher frequency and disappears at 0.628 rad/s (see Supporting Information). Experiments with the linear triblock copolymer $PS_{27}$-$PAA_{139}$-$PS_{27}$ show the gel to give similar response as the star polymers with shorter blocks−long linear response together with strain hardening.

The strain response of the solutions may be classified to represent "strong" and "weak" gels.[2] The strong gels are the ones where a significant linear region is observed together with the strain hardening while weak gels are characterized by narrow linear region and strong shear thinning. The linear regime and the strain hardening in the case of associating polymers have been explained by simultaneous contribution of the change in the conformation of the hydrophilic block together with the

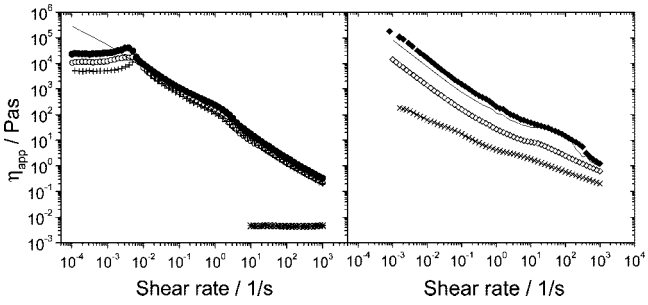


**Figure 4.** Flow curves of polymer solutions at 20 °C. Polymer solutions; on the left $(PAA_{64})_4$ (34 g/L, *), $(PAA_{64}$-*b*-$PS_{15})_4$ (22 g/L, +; 30 g/L,○; 34 g/L, ●, line ramping shear rate down) and on the right $(PAA_{58}$-*b*-$PS_{20})_4$ (19 g/L, ×; 22 g/L, ◇; 34 g/L, ◆; line ramping shear rate down).

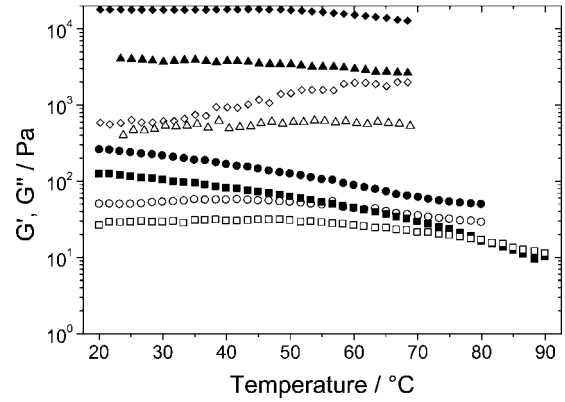


**Figure 5.** Oscillatory temperature sweeps of polymer solutions: $(PAA_{58}$-*b*-$PS_{20})_4$ ($C_p$ = 34 g/L; $G'$, ◆; $G''$, ◇); $(PAA_{64}$-*b*-$PS_{17})_4$ ($C_p$ = 34 g/L; $G'$, ▲; $G''$, Δ); $(PAA_{64}$-*b*-$PS_{15})_4$ ($C_p$ = 34 g/L; $G'$, ●; $G''$, ○); and $(PAA_{64}$-*b*-$PS_{15})_4$ ($C_p$ = 30 g/L; $G'$, ■; $G''$, □).

strain induced dissociation of the intermolecular hydrophobic associating groups. Breedveld et al.[41] reported similar experiments as in the present study for poly-L-lysine-*b*-poly-L-leucine diblock copolypeptide solutions where the overall length of the polymers were kept similar, but the lengths of the hydrophilic L-lysine and hydrophobic L-leucine blocks were varied. It was observed that increasing the hydrophobe length led to similar behavior as in the present case. Polymer with short hydrophobic blocks, 20 monomer units of L-leucine, showed strain hardening behavior and a linear regime extending to large strains. Increasing the poly-L-leucine block to 30 or 40 monomer units led to more brittle gels with increased modulus and shorter linear regime. This behavior was attributed to the deformability of the gels—longer hydrophobes result in a more rigid structure that breaks easily. The same explanation applies to the polymers in the present case, where shorter PS blocks allow the sample to deform to a larger extent before it yields.

It should also be noted that in the case of poly(*tert*-butyl acrylate), poly(2-vinylpyridine) (P2VP), and poly(acrylic acid) triblock copolymers, (P*t*BA-P2VP-P*t*BA) and (PAA-P2VP-PAA),[12] as well as in the case of poly-L-lysine-*b*-poly-L-leucine[41] the strain hardening amplitude for "strong" gels seems to be rather independent of the polymer used and occurs at around 100% strain at the used oscillation frequency (6.28 or 3.14 rad/s). In the present study we varied the frequency from 0.628 to 62.8 rad/s to probe the behavior at different frequencies and also monitored the behavior at different concentrations. It was observed that for the "strong" gels the onset and the magnitude of strain hardening was independent of the frequency used. Increasing the concentration to 30 g/L or above showed a mixed behavior, less pronounced strain hardening, and simultaneous shear thinning. On the other hand, for the "weak" gels increasing the frequency from 0.1 to 1 and 10 Hz made the shoulder at higher strains to become more pronounced, while increase in concentration did not affect the onset of the linear regime.

**Steady Shear.** Viscosity measurements under steady shear are another way to probe the rheological response of the solutions. In Figure 4 the steady shear properties of the samples above the gelation threshold for solutions of $(PAA_{64}$-*b*-$PS_{15})_4$ and $(PAA_{58}$-*b*-$PS_{20})_4$ are shown. The solutions of $(PAA_{64}$-*b*-$PS_{17})_4$ gave qualitatively similar results as the solutions of $(PAA_{58}$-*b*-$PS_{20})_4$, in agreement with the oscillatory studies.

As seen from the graph on the left, the hydrolyzed star polyelectrolyte without hydrophobes, $(PAA_{64})_4$, at a comparable concentration (34 g/L), does not give a noticeable rise to viscosity but instead the viscosity is very close to that of water. This means that the unhydrolysed *t*BA units (~3%), which most likely are either randomly distributed along the chains or situated in the crowded core of the star, do not produce similar junction points as longer PS blocks and hence do not enhance the viscosity.

As seen from Figure 4, clear differences between the samples with shorter and longer PS blocks are encountered. The flow curves of $(PAA_{64}$-*b*-$PS_{15})_4$ solutions have a detectable plateau at low shear rates and would enable the calculation of zero-shear viscosity. However, upon ramping the shear rate down the plateau is lost and does not recover until the sample is stabilized, which means that the structure changes due to shearing. The $(PAA_{64}$-*b*-$PS_{17})_4$ and $(PAA_{58}$-*b*-$PS_{20})_4$ above gelation threshold, on the other hand, show no plateau even at very low shear rates. Rather unexpectedly, very little hysteresis is seen in the curves, and ramping the shear up, down, and up again produces very similar curves. Increasing the concentration does not increase the viscosity substantially for the solutions of polymers with long stickers, 17 or 20 PS units, in correlation with the oscillatory studies where the gel structure is easily broken by shearing. It should however be noted that the associative nature of the solutions is displayed in the flow curves as a slight upward turn at 10−100 1/s, an indication of the breakup of the transient associations.

**Effect of Temperature on the Rheological Behavior.** The properties of the gels upon heating were probed via oscillatory measurements using oscillation frequency of 6.28 rad/s in the linear regime and heating the gels at 1 °C/min. Hydrogels of $(PAA_{54}$-*b*-$PS_6)_4$ turned to viscous liquids upon heating depending on the concentration of the solution,[33] and thus it was of interest to probe the effect for the polymers having longer hydrophobic blocks. From the concentrated solutions of the star polymers with longer hydrophobes it can be observed that only moderate softening of the gels takes place. By lowering the concentration and heating the gel to 90 °C, the solution with $(PAA_{64}$-*b*-$PS_{15})_4$ at a concentration of 30 g/L shows that the sample undergoes a gel to solution transition at 80 °C, shown in Figure 5, while no crossover was noticed for the star polymers having 17 or 20 units long PS stickers. The behavior of $(PAA_{64}$-*b*-$PS_{15})_4$ is similar as with $(PAA_{54}$-*b*-$PS_6)_4$; i.e., the increasing temperature increases the molecular motions and leads to faster exchange rate of the transient junctions. On the other hand, solutions of polymers with longer stickers obviously have tighter associations and thus less exchange due to increased thermal motion in the studied range takes place. However, some decrease of moduli takes place with heating with no signs of thermothickening. Thermothickening has recently been reported to occur for example with an amphiphilic polyampholeyte based on poly(2-vinylpyridine) (P2VP) and poly(acrylic acid) triblock copolymer $PAA_{135}$-$P2VP_{628}$—$PAA_{135}$[26] or with thermoresponsive stereoblock polymers of PNIPAM[38] in aqueous solutions.

**SAXS Studies of the Gels.** Small-angle X-ray scattering (SAXS) was used to probe the structure of the polymer solutions

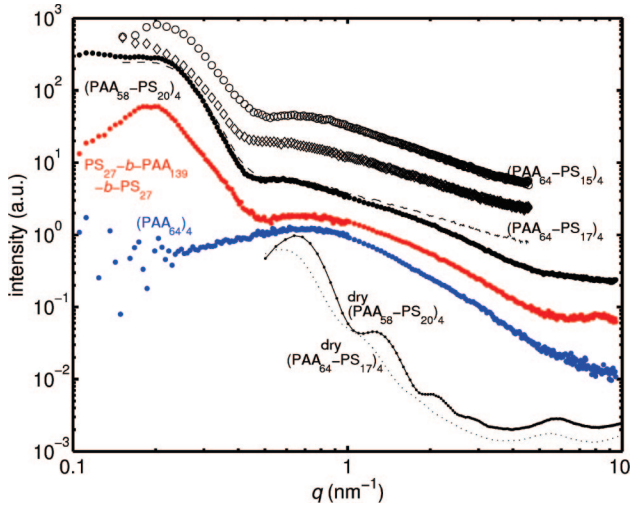


**Figure 6.** Measured X-ray scattering curves for solid and aqueous 35 g/L polymer solutions. The curves are measured with various sample-to-detector distances of 20, 50, and 140 cm and combined in some cases. The curves are offset for clarity. From top to bottom: star-$(PAA_{64}$-$b$-$PS_{15})_4$ (circles), star-$(PAA_{64}$-$b$-$PS_{17})_4$ (diamonds), star-$(PAA_{58}$-$b$-$PS_{20})_4$ (dashed) and (dots, measured 1 month later), triblock ($PS_{27}$-$b$-$PAA_{139}$-$b$-$PS_{27}$) (dots), star-$(PAA_{64})_4$ (dots), dried star-$(PAA_{58}$-$b$-$PS_{20})_4$ (dot-line), and dried star-$(PAA_{64}$-$b$-$PS_{17})_4$ (dotted line).

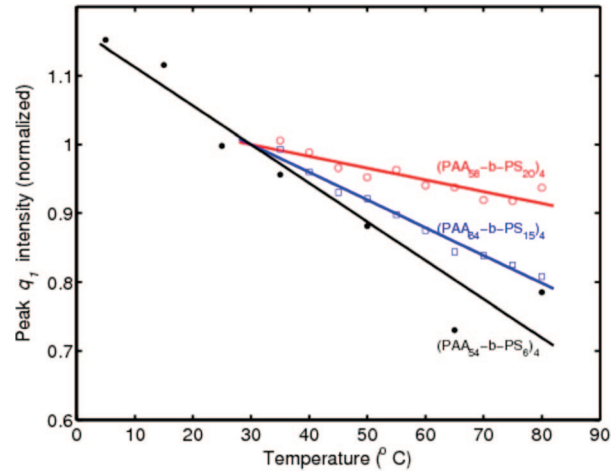


**Figure 7.** Evolution of intensity of the first maximum at $q_1^* \sim 0.2$ $nm^{-1}$ as a function of temperature: star-$(PAA_{58}$-$b$-$PS_{20})_4$ (circles), star-$(PAA_{64}$-$b$-$PS_{15})_4$ (squares), and star-$(PAA5_4$-$b$-$PS_6)_4$ (dots). The data for $N_{PS} = 17$ was similar to $N_{PS} = 15$ and is omitted for clarity. Lines are to guide the eye.

in the hydrogel state, i.e., at $C_p = 35$ g/L. Three star-block copolymers polymers, $(PAA_{64}$-$b$-$PS_{15})_4$, $(PAA_{64}$-$b$-$PS_{17})_4$, and $(PAA_{58}$-$b$-$PS_{20})_4$, were inspected with triblock $PS_{27}$-$b$-$PAA_{139}$-$b$-$PS_{27}$ and core homopolymer star measured for comparison. Figure 6 shows scattering intensity at $C_p = 35$ g/L, at which concentration all the samples except $(PAA_{64})_4$ are in the hydrogel state. In case of copolymer samples, two peaks at $q_1^* = 0.2$ $nm^{-1}$ and $q_2^* = 0.8$ $nm^{-1}$ can be observed, whereas $(PAA_{64})_4$ shows only the latter maximum. The scattering patterns are very similar to what was obtained before[33] for a shorter sticker length $(PAA_{54}$-$b$-$PS_6)_4$, except there the peaks occurred at somewhat higher scattering angles, at $q_1^* = 0.35$ $nm^{-1}$ and $q_2^* = 1.0$ $nm^{-1}$.

A broad intensity maximum within the $q$ range 0.1−1 $nm^{-1}$ is generally observed for solutions of charged polyelectrolytes. These are thought to originate from interchain correlations, where individual chains try to separate as far as possible thus leading to a broad "correlation hole" peak (also known as the Coulomb peak). The peak position $q^*$ corresponds to nearest chain distance $2\pi/q^*$ and is directly related to concentration. The peak position scales as $q^* \sim c^{1/3}$ below the chain overlap concentration but shifts to $q^* \sim c^{1/2}$ when the chains are forced much closer than their length.[44] For a linear PAANa, of weight 30 000 g/mol, for example, overlap is expected above $c^* = 1-2$ mg/mL, but for the 4-star morphology the threshold concentration may be a factor 5−10 higher.[45] Noteworthy, homopolymer $(PAA_{64})_4$ shows only one maximum at $q_2^* = 0.8$ $nm^{-1}$. Thus, we ascribe this peak to correlation between PAA chains in the aqueous solution. We did not measure concentration series, but the maximum seems to be in excellent accord with that by Moinard et al.[45] for the same type of stars. Therein, the peak position scaled as $q_2^* \sim c^{1/2}$ so we should expect the same behavior here.

As fas as peak $q_1^*$ goes, block copolymers, e.g., diblock PAA−PS,[23] are known to show maxima due to intermicellar interference. In dilute solutions, diblock polymers form spherical aggregates where hydrophobic blocks constitute the core and the polyelectrolyte block is dispersed in the corona. Various cubic ordered structures are obtained at higher concentrations (few 10 g/L),[46] especially under shear. However, using multiarm (high $f$) block copolymers ordered morphologies are obtained at significantly lower concentrations.[47] Increasing concentration further to the point of drying the sample, cylindrical and lamellar order morphologies might eventually appear (cf. Figure 6).

The first maximum at $q_1^* \sim 0.2$ $nm^{-1}$ is therefore explained as interference between regions of polystyrene in the water/PAA matrix. The peak positions give the average intermicellar distances (calculated as Bragg distances), which are 18 nm (for $N_{PS} = 6$),[33] 26 nm (for $N_{PS} = 15$), 27 nm (for $N_{PS} = 17$), 28 nm (for $N_{PS} = 20$), and 30 nm (for $N_{PS} = 27$ triblock sample). From these we obtain rough estimates for the aggregation number (number of PS stickers per micelle) $N_{agg} = 21$, 47, 57, 60, and 58 for $N_{PS} = 6$, 15, 17, 20, and 29 (triblock), respectively. This calculations assume bulk density for the spherical PS domains which organize in a simple cubic lattice. The increase of $N_{agg}$ with $N_{PS}$ seems logical: The size of PS domains competes with chain density. The average distance between PAA chains at the surface of PS sphere is $1.14N_{PS}^{1/3}/N_{agg}^{1/6}$ nm. Thus, for fixed PAA density $N_{agg}$ would tend to grow as square of the sticker length $N_{PS}$ and consequently the radius (roughly $0.34(N_{agg}N_{PS})^{1/3}$ nm) more or less linearly with $N_{PS}$. Functionality is also a factor: the triblock sample despite larger $N_{PS}$ had the same aggregation number as the star polymer. Korobko et al., on the other hand, obtained $N_{agg} = 100$ for a similar diblock copolymer $PAA_{80}$-$b$-$PS_{20}$.[23]

The overall picture comprises solid PS core islands in a surrounding sea of interpenetrating PAA arms. This resembles sodium polystyrenesulfonate (NaPSS) studied by Heinrich et al.[48] where the role of the aggregate is taken by stars with higher functionality ($f = 10-12$). We stress that we cannot see the PS domains directly from the scattering curves; the small-angle scattering from the domains is masked off by the interference maximum $q_1^*$. Solid PS, on the other hand, produces a faint maximum at $q = 6$ $nm^{-1}$.This is seen in the solid samples of Figure 6, but in the solutions the overall PS fraction is too small to allow detection of the PS phase. In view of structure vs rheological behavior, we do not see the gross differences in morphology or order between samples of different sticker length $N_{PS}$ or functionality $f$. Indirectly, we observe both increased domain size and aggregation with increasing sticker length, both of which are expected to increase the moduli due to stronger and denser cross-linking.

The evolution of the SAXS intensity patterns was also followed as a function of temperature up to 80 deg. A slight decrease in intensity with increasing temperature is observed though not nearly as great as previously obtained for the sample $N_{PS} = 6$. In Figure 7 the intensity of the first maximum $I(q_1^*)$ is plotted as a function of $T$. The data are normalized to

$I(q_2^*)$ and to unity at 30 deg to better allow comparison without considering possible evaporation and changes in scattering contrast due to thermal expansion. The results show increased resilience to thermal disordering with longer PS stickers.

## Conclusions

Water-dispersible amphiphilic star polymers with four arms based on poly(acrylic acid) (PAA) cores and variable size polystyrene (PS) hydrophobes at the ends of the arms were synthesized and their rheological properties studied in aqueous solutions. In water the polymers form hydrogels with increasing polymer concentration ($C_p$). The gelling concentration in water was found to be around 20 g/L, and elastic gels with increasing plateau modulus with increasing length of the PS block were formed. The observed physical network formation at such low concentrations was rationalized by the transient intermolecular hydrophobic association of the PS blocks and the starlike topology of the polymers. Comparison with a linear triblock copolymer with PS end blocks having comparable molar mass and PS−PAA ratio showed that the branched topology of the star polymers results in more effective network formation and gels with higher elasticity.

The polymer solutions with shorter hydrophobes, 15 PS units in each arm, showed strain hardening behavior at increasing oscillatory strain, indicating the formation of "strong" gels. The solutions of polymers with longer PS stickers, 17 or 20 PS units, formed "weak" gels characterized by short linear viscoelastic region followed by strong shear thinning. The gel structure affected also the behavior in steady shear, leading to more shear thinning gels in the case of longer hydrophobic stickers. Upon heating the solutions of polymers with shorter PS block showed gel-to-solution transition provided that the concentration was low enough, while the polymers with longer hydrophobes, 17 or 20 PS units, do not soften as much. This behavior is rationalized by the tighter associations between the longer PS blocks compared with the more mobile shorter PS blocks.

Small-angle X-ray experiments showed two distinct scattering correlation peaks for samples above the gelling $C_p$. These were interpreted in terms of a hierarchical model with hydrophobic aggregates and interspersed sodium polyacrylate. It was deduced that the hydrophobe aggregate size grows due to both increased sticker length and increased number of chains per aggregate.

The results indicate that small differences in the structure of associating polymers may result in large differences in the resulting hydrogel properties, and precise synthesis of polymers is a necessity for making hydrogels with desired properties.

**Acknowledgment.** S. Strandman thanks the Finnish National Graduate School in Nanoscience (NGS-NANO) for funding. Perstorp Polyols, Sweden, is acknowledged for kindly supplying ditrimethylolpropane.

**Supporting Information Available:** Table of molar masses of starlike and linear block copolymers; figures of size exclusion chromatograms, oscillatory frequency sweeps, and oscillatory strain sweeps for precursors of starlike and linear block copolymers. This material is available free of charge via the Internet at http://pubs.acs.org.

## References and Notes

(1) Glass, J. E., Ed. *Hydrophilic Polymers: Performance with Environmental Acceptability*; Advances in Chemistry Series 248; American Chemical Society: Washington, DC, 1996.
(2) Kajiwara, K., Osada, Y., Eds. *Gels Handbook*; Academic Press: San Diego, CA, 2001.
(3) Bhatia, S. R.; Mourchid, A.; Joanicot, M. *Curr. Opin. Colloid Interface Sci.* **2001**, *6*, 471–478.
(4) Kimerling, A. S.; Rochefort, W. E.; Bhatia, S. R. *Ind. Eng. Chem. Res.* **2006**, *45*, 6885–6889.
(5) Cohen Stuart, M. A.; Hofs, B.; Voets, I. K.; de Keizer, A. *Curr. Opin. Colloid Interface Sci.* **2005**, *10*, 30–36.
(6) Annable, T.; Buscall, R.; Ettelaie, R. *Colloids Surf., A* **1996**, *112*, 97–116.
(7) Tirtaatmadja, V.; Tam, K. C.; Jenkins, R. D. *Macromolecules* **1997**, *30*, 1426–1433.
(8) Tam, K. C.; Jenkins, R. D.; Winnik, M. A.; Bassett, R. A. *Macromolecules* **1998**, *31*, 4149–4159.
(9) Ma, S. X.; Cooper, S. L. *Macromolecules* **2001**, *34*, 3294–3301.
(10) Ma, S. X.; Cooper, S. L. *Macromolecules* **2001**, *35*, 2024–2029.
(11) Park, S. Y.; Han, D. K.; Kim, S. C. *Macromolecules* **2001**, *34*, 8821–8824.
(12) Stavrouli, N.; Aubry, T.; Tsitsilianis, C. *Polymer* **2008**, *49*, 1249–1256.
(13) Vermonden, T.; Besseling, N. A. M.; van Steenbergen, M. J.; Hennink, W. E. *Langmuir* **2006**, *22*, 10180–10184.
(14) Xue, W.; Hamley, I. W.; Castelletto, V.; Olmsted, P. D. *Eur. Polym. J.* **2004**, *40*, 47–56.
(15) Kujawa, P.; Audibert-Hayet, A.; Selb, J.; Candau, F. *J. Polym. Sci., Part B: Polym. Phys.* **2004**, *42*, 1640–1655.
(16) Kujawa, P.; Audibert-Hayet, A.; Selb, J.; Candau, F. *Macromolecules* **2006**, *39*, 384–392.
(17) Tam, K. C.; Farmer, M. L.; Jenkins, R. D.; Bassett, D. R. *J. Polym. Sci., Part B: Polym. Phys.* **1998**, *36*, 2275–2290.
(18) Borrega, R.; Tribet, C.; Audebert, R. *Macromolecules* **1999**, *32*, 7798–7806.
(19) Tsitsilianis, C.; Iliopoulos, I.; Ducouret, G. *Macromolecules* **2000**, *33*, 2936–2943.
(20) Tsitsilianis, C.; Katsampas, I.; Sfika, V. *Macromolecules* **2000**, *33*, 9054–9059.
(21) Tsitsilianis, C.; Iliopoulos, I. *Macromolecules* **2002**, *35*, 3662–3667.
(22) Cadix, A.; Chassenieux, C.; Lafuma, F.; Lequeux, F. *Macromolecules* **2005**, *38*, 527–536.
(23) Korobko, A. V.; Jesse, W.; Lapp, A.; Egelhaaf, S. U.; van der Maarel, J. R. C. *J. Chem. Phys.* **2005**, *122*, 024902.
(24) de la Fuente, J. L.; Wilhelm, M.; Spiess, H. W.; Madruga, E. L.; Fernandez-Garcia, M.; Cerrada, M. L. *Polymer* **2005**, *46*, 4544–4553.
(25) Antunes, F. E.; Lindman, B.; Miguel, M. G. *Langmuir* **2005**, *21*, 10188–10196.
(26) Bossard, F.; Tsitsilianis, C.; Yannopoulos, S. N.; Petekidis, G.; Sfika, V. *Macromolecules* **2005**, *38*, 2883–2388.
(27) Angelopoulos, S. A.; Tsitsilianis, C. *Macromol. Chem. Phys.* **2006**, *207*, 2188–2194.
(28) Gotzamanis, G. T.; Tsitsilianis, C.; Hadjiyannakou, S. C.; Patrickios, C. S.; Lupitskyy, R.; Minko, S. *Macromolecules* **2006**, *39*, 678–683.
(29) Podhajecka, K.; Prochazka, K.; Hourdet, D. *Polymer* **2007**, *48*, 1586–1595.
(30) Bossard, F.; Aubry, T.; Gotzamanis, G.; Tsitsilianis, C. *Soft Matter* **2006**, *2*, 510–516.
(31) Li, Y.; Tang, Y.; Narain, R.; Lewis, A. L.; Armes, S. P. *Langmuir* **2005**, *21*, 9946–9954.
(32) Li, Y.; Narain, R.; Ma, Y.; Lewis, A. L.; Armes, S. P. *Chem. Commun.* **2004**, 2746–2747.
(33) Hietala, S.; Mononen, P.; Strandman, S.; Järvi, P.; Torkkeli, M.; Jankova, K.; Hvilsted, S.; Tenhu, H. *Polymer* **2007**, *48*, 4087–4096.
(34) Durand, A.; Hourdet, D. *Polymer* **1999**, *40*, 4941–4951.
(35) Masunaka, H.; Sasaki, K.; Akiba, I. *J. Macromol. Sci., Phys.* **2004**, *43*, 1063–1073.
(36) Kujawa, P.; Watanabe, H.; Tanaka, F.; Winnik, F. M. *Eur. Phys. J.* **2005**, *E17*, 129–137.
(37) Tang, T.; Castelletto, V.; Parras, P.; Hamley, I. W.; King, S. M.; Roy, D.; Perrier, S.; Hoogenboom, R.; Schubert, U. S. *Macromol. Chem. Phys.* **2006**, *207*, 1718–1726.
(38) Hietala, S.; Nuopponen, M.; Kalliomäki, K.; Tenhu, H. *Macromolecules* **2008**, *41*, 2627–2631.
(39) Zhao, G.; Chen, S. B. *J. Colloid Interface Sci.* **2007**, *316*, 858–866.
(40) Kjøniksen, A.-L.; Nyström, B.; Lindman, B. *Macromolecules* **1998**, *31*, 1852–1858.
(41) Breedveld, V.; Nowak, A. P.; Sato, J.; Deming, T. J.; Pine, D. J. *Macromolecules* **2004**, *37*, 3943–3953.
(42) Jankova, K.; Bednarek, M.; Hvilsted, S. *J. Polym. Sci., Part A: Polym. Chem.* **2005**, *43*, 3748–3759.
(43) Matyjaszewski, K.; Miller, P. J.; Pyun, J.; Kickelbick, G.; Diamanti, S. *Macromolecules* **1999**, *32*, 6526–6535.
(44) Wang, L.; Bloomfield, V. A. *Macromolecules* **1991**, *24*, 5791–5795.
(45) Moinard, D.; Taton, D.; Gnanou, Y.; Rochas, C.; Borsali, R. *Macromol. Chem. Phys.* **2003**, *204*, 89–97.
(46) Prud'homme, R. K.; Wu, K.; Schneider, D. K. *Langmuir* **1996**, *12*, 4651–4659.
(47) Furukawa, T.; Ishuzu, K. *Macromolecules* **2003**, *36*, 434–439.
(48) Heinrich, M.; Rawiso, M.; Zilliox, J. G.; Lesieur, P.; Simon, J. P. *Eur. Phys. J. E* **2001**, *4*, 131–142.

MA801805Q